Numerical Modelling of Wind Flow over Hills

O. Agafonova, A. Koivuniemi, B. Conan, A. Chaudhari, H. Haario, and J. Hamalainen

Abstract The paper demonstrates when the Wind Atlas Analysis and Application Program (WAsP) is comparable to Computational Fluid Dynamics (CFD) in order to use the WAsP wind prediction later for time consuming CFD simulations. Three different numerical methods (WAsP, RANS, LES) for observation of wind flow over the hills are described and compared with the wind-tunnel experiment. The paper shows that WAsP provides reasonably realistic results for the flow over the commonly found in nature shallow hills.

Keywords Flow over hills • LES • RANS • Turbulence • WAsP • Wind tunnel experiment

1 Introduction

Numerical modelling of atmospheric flows over a complex terrain is an important problem for wind energy applications, since it helps in arrangement, installation and control of the on-shore wind farms. The research subject is a justification of possible use of WAsP as prediction for the precise and time consuming CFD for a complex terrain. This is our second paper devoted to WAsP and CFD comparison for a wind flow over two-dimensional hills. In the first study [2], two hills (Hill3 and Hill5) from Castro and Apsley [5] were studied numerically and compared with the well known RUSHIL wind tunnel experiment [9]. The expected agreement was obtained for those hills [2]. In the present work, we continue to study the wind flow over two-dimensional hills as it represents the simplest flow over a complex terrain. Earlier, experiments for the hill flow were conducted using the hot-wired anemometry methodology. This time, we study the same shape of hills but with different slopes (Hill2 and Hill4). Meanwhile, computational results for these particular hills are compared with PIV measurements. At the same time, these hills are interesting for comparison because Hill2 has a very high slope and Hill4 is a borderline case

O. Agafonova (✉) • A. Koivuniemi • B. Conan • A. Chaudhari • H. Haario • J. Hamalainen
Lappeenranta University of Technology, P.O. Box 20, FI-53851 Lappeenranta, Finland
e-mail: oxana.agafonova@lut.fi

because of the reattachment zone beyond the hill. In addition, these two hills have not been studied enough neither numerically nor experimentally.

The equations, which describe the shape of the hills, are given in [1, 5]. The average slope of hills n $\left(n = \frac{H}{a}, a \text{ is half length and } H\text{—the height of the hill}\right)$ are equal to 0.5 and 0.25. In present study, these hills are named as Hill2 and Hill4 respectively. The experiment for Hill2 and Hill4 was conducted in the VKI-L2 wind tunnel of the von Karman Institute for Fluid Dynamics using the Particle Image Velocimetry (PIV) methodology. The hills were fabricated in wood in similarity with the RUSHIL experiment. The Reynolds number, based on the hill height, used in experiments is around 17,000. The inlet velocity and turbulence profiles of the experiment are detailed in Conan [8].

2 Mathematical Modelling

The equations of motion for a viscous incompressible liquid (Navier-Stokes Equations) without body forces are obtained from the integral laws of mass and momentum conservation and are written in the form [1]:

$$\begin{cases} \nabla \cdot \mathfrak{v} = 0 \\ \rho \dfrac{d\mathfrak{v}}{dt} = -\nabla p + \mu \nabla^2 \mathfrak{v} \end{cases}$$

In scalar-tensor form the system of Navier-Stokes equations takes the following appearance:

$$\frac{\partial u_i}{\partial x_i} = 0; \tag{1}$$

$$\frac{\partial u_i}{\partial t} + u_j \frac{\partial u_i}{\partial x_j} = -\frac{1}{\rho} \frac{\partial p}{\partial x_i} + \frac{1}{\rho} \frac{\partial}{\partial x_j} t_{ij}. \tag{2}$$

Then, using Eqs. (1), (2) can be rewritten in the form (3):

$$\frac{\partial u_i}{\partial t} + \frac{\partial}{\partial x_j}(u_j u_i) = -\frac{1}{\rho} \frac{\partial p}{\partial x_i} + \frac{1}{\rho} \frac{\partial}{\partial x_j} t_{ij}. \tag{3}$$

The components t_{ij} of the viscous stress tensor are equal to $t_{ij} = 2\mu s_{ij}$, where s_{ij} are the components of the strain-rate tensor $s_{ij} = \frac{1}{2}(\frac{\partial u_j}{\partial x_i} + \frac{\partial u_i}{\partial x_j})$.

Using the Reynolds averaging [12], the velocity component u_i can be represented in the form $u_i = U_i + u_i'$, where U_i and u_i' are mean and fluctuating components

respectively. Therefore, Eq. (1) leads to:

$$\frac{\partial U_i}{\partial x_i} = 0; \quad \frac{\partial u_i'}{\partial x_i} = 0. \tag{4}$$

Applying the averaging operation to Eq. (3), we obtain the Reynolds-averaged Navier-Stokes (RANS) equation:

$$\frac{\partial}{\partial t}(\rho U_i) + \frac{\partial}{\partial x_j}(\rho U_j U_i) = -\frac{\partial p}{\partial x_i} + \frac{\partial}{\partial x_j}(\overline{\tau_{ij}} - \rho \overline{u_j' u_i'}), \tag{5}$$

where $\overline{\tau_{ij}} = 2\mu S_{ij}$ and $\rho \overline{u_j' u_i'}$ are the components of the viscous stress tensor and the Reynolds-stress tensor respectively.

Large Eddy Simulation (LES) is a computational technique in which the large eddies are computed and the smallest eddies are modelled. Using the filtration concept that is applying the volume-average filter to the original Navier-Stokes equations, the velocity component u_i can be written in the form $u_i = \overline{u}_i + u_i'$, where $\overline{u}_i$, u_i' denote the resolvable-scale filtered and subgrid scale (SGS) components respectively. For an incompressible flow, the continuity and Navier-Stokes equations assume the following form [12] :

$$\frac{\partial \overline{u}_i}{\partial x_i} = 0; \tag{6}$$

$$\frac{\partial \overline{u}_i}{\partial t} + \frac{\partial \overline{u_i u_j}}{\partial x_j} = -\frac{1}{\rho}\frac{\partial \overline{p}}{\partial x_i} + \nu \frac{\partial^2 \overline{u}_i}{\partial x_k \partial x_k}. \tag{7}$$

The WAsP equations are based on a linearization of the Navier-Stokes equations of motion. The second order terms of the Navier-Stokes equations are ignored in the solution, leading to the simple steady equations [10]:

$$\frac{\partial u_i}{\partial x_i} = 0; \tag{8}$$

$$u_{j0}\frac{\partial u_i}{\partial x_j} = -\frac{1}{\rho}\frac{\partial p}{\partial x_i} + \frac{1}{\rho}\frac{\partial}{\partial x_j}t_{ij}, \tag{9}$$

where the velocities $(u_{10}, u_{20}, 0)$ are the components of the initial wind vector $\mathfrak{v}_0$. The flow is modeled as horizontal flow perturbations of u and is independent of the real wind velocity. This can be done using potential flow

$$u = \nabla \chi. \tag{10}$$

The boundary conditions for the model are such that the potential flow is zero far away from the point of interest

$$\nabla \chi|_{r=R} = 0, \tag{11}$$

and the flow is parallel to the ground surface

$$u_{30} = \left. \frac{\partial \chi}{\partial z} \right|_{z=0} = \overline{u}_0 \cdot \nabla h(r, \phi). \tag{12}$$

In the WAsP program the solution is derived by expressing the equation in cylindrical coordinates and writing the solution in a series of J-Bessel functions.

3   Numerical Modelling

The steady state problem is solved numerically using the CFD technique for different hill slopes. The finite-volume meshes for RANS simulations are created using the Gambit software and the total number of cells is 300,800 elements in each case. The minimum control volume dimension is $0.05\,H \times 0.00205\,H$ at the hill summit and is extended upwind and downwind uniformly, and vertically with expansion ratio of 1.025 using a geometric progression method. RANS equations are solved numerically using the ANSYS FLUENT software by applying the SST $k - \omega$ turbulence model with the so-called "Low Reynolds Corrections" treatment near the wall [3]. The inlet velocity profile used for the computation is logarithmic (for details see [5]). The inflow boundary conditions for the turbulent kinetic energy and the specific dissipation rate are obtained from the periodic flow simulations over the flat terrain of the same size as the computation domain for hill simulations.

In addition to RANS simulations, several LES calculations are also carried out for both Hill2 and Hill4. For this purpose, the 2D hill geometry is extruded in the spanwise direction in order to perform 3D LES (see Fig. 2). The finite volume mesh consisting of 7,875,000 cells is used for the LES simulation. The minimum control volume size at the hill summit is $0.125\,H \times 0.0031\,H \times 0.137\,H$ in x, y and z directions, respectively. The standard Smagorinsky sub-grid scale model is used to model the smaller eddies. The mapping technique was used at the inlet boundary in order to generate the realistic upstream boundary layer for LES, as explained in [6]. Recently, we have used the recycling technique in LES for Hill3 [2, 7].

The LES computations for both hills are run with the automatic time-step by fixing the maximum Courant number to $Cu = 0.25$ until the physical time $t = 40\,s$ is reached. Then, they are time averaged with all quantities over the last $30\,s$. In addition to time averaging, the results are also space averaged over the span-wise direction.

WAsP maps that describe similar hills are created for comparison with CFD. WAsP simulations are performed at real scale. The height of the hills is taken as

117 m and the computational domain is extended up to 1 km in vertical direction. Surface roughness is similar to RANS modelling. The flow-model parameters are configured in order to model a neutrally stratified situation. The actual flow is examined with reference sites along the stream-wise axis of the hill.

4 Results and Discussions

In this study the finite-volume method based open source OpenFOAM 2.2.2 and commercial ANSYS FLUENT 13.0 software are employed for LES and RANS calculations, correspondingly.

Figure 1 shows the mean velocity in stream-wise direction from the experiment for the steep hill. The size of the recirculation x/H can be estimated between 3.5 and 4.5.

Experimental results for Hill4 did not show the reverse flow beyond the hill. At the same time, the separation region for this hill was detected by both RANS and LES approaches (see Figs. 2 and 3b). In the case of RANS, the reattachment point is $x_r = 5.216$ H. The reattachment point predicted by LES is $x_r = 6.58$ H. In fact,
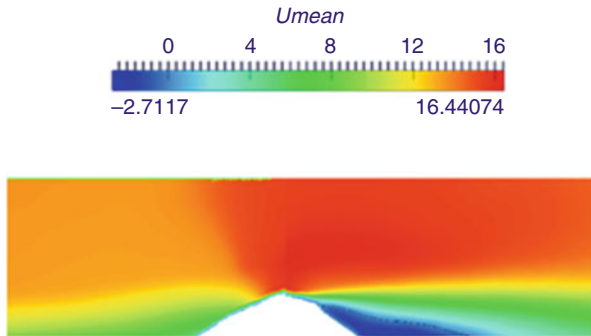

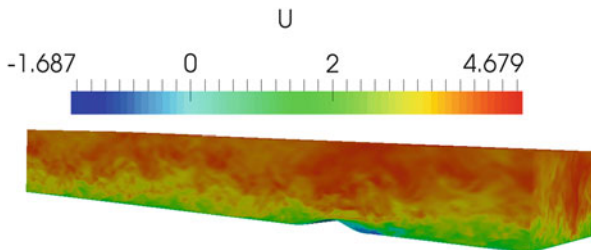**Fig. 1** Mean velocity [m/s] in stream-wise direction from the experiment [8] for Hill2

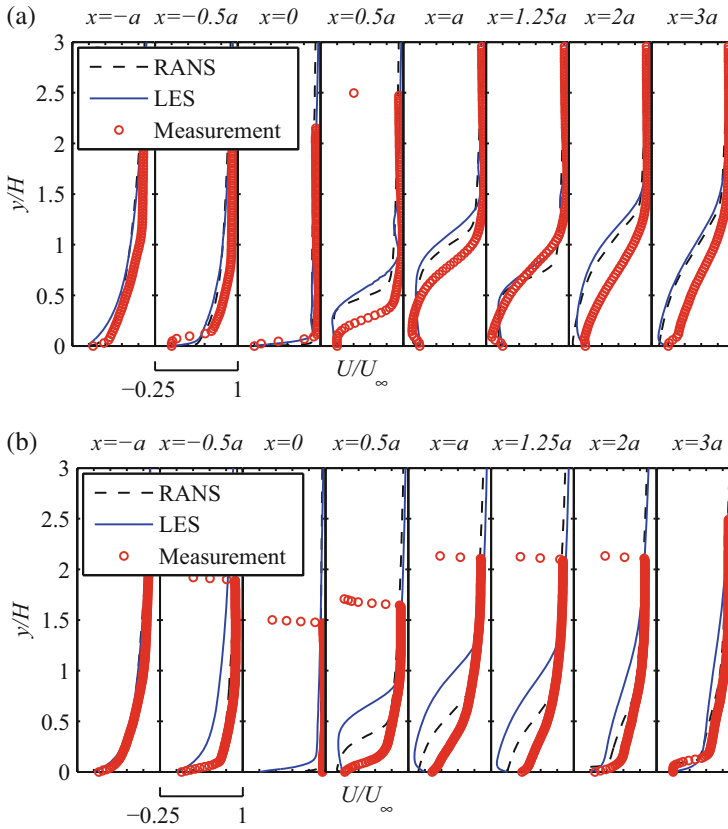**Fig. 2** Instantaneous velocity [m/s] in stream-wise direction from the simulation for Hill4

Fig. 3 Vertical profiles of the mean stream-wise velocity (U/U_∞) compared with measurements for the flow over Hill2 (**a**) and Hill4 (**b**) at certain longitudinal locations

the reattachment length in the experiment by Loureiro et al. [11] for a shallower hill (average slope is 0.2) than Hill4 equals 6.67 H.

Figure 3a, b show the vertical profiles of the stream-wise velocity compared with the measurements. The current RANS agrees with the experiment well enough for Hill2 (see Fig. 3a). Both RANS and LES underestimate the wind velocity in the separation region of Hill2.

It can be seen in Fig. 4a that WAsP significantly differs and overestimates the wind velocity in reattachment region of steep Hill2. However, Fig. 4b shows that WAsP agrees well enough for the shallow hill (Hill4) except the separation region, in which WAsP slightly overestimates the velocity.
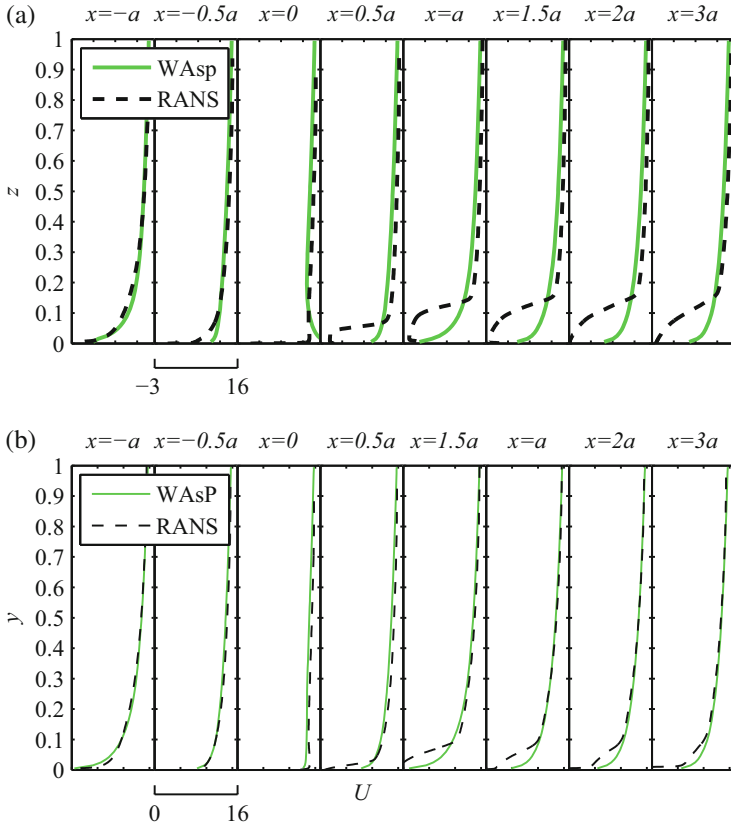
Fig. 4 Vertical profiles of the mean stream-wise velocity (U, [m/s]) compared with RANS for the flow over Hill2 (**a**) and Hill4 (**b**) at certain longitudinal locations

5 Conclusions

In the current study, we carried out WAsP, RANS and LES to investigate the turbulent flows over two-dimensional hills with different slopes. The results of RANS and LES simulations were described and compared with available experimental data. The obtained RANS results agree relatively well with LES and measurements and might be used for later validation of WAsP results.

WAsP produces reasonably realistic results for the flow over the shallow hills which are commonly found in nature (see Fig. 4b) and corresponds well with the other studies [2, 4].

This research work shows that the WAsP wind prediction agrees relatively well with RANS and can be used as an inflow for performing later RANS simulations over the real-scale and complex wind park terrain with shallow hills, forest and wind turbines.

References

1. Agafonova, O.: Computational and experimental study of an air flow over a hill. Master thesis, Lappeenranta (2011)
2. Agafonova, O., Koivuniemi, A., Chaudhari, A., Haario, H., Hamalainen J.: Limits of WAsP modelling in comparison with CFD for wind flow over two-dimensional hills. In: Proceedings of EWEA 2014 Annual Event, Europe's Premier Wind Energy Event, Barcelona, Spain (2014)
3. Ansys Fluent Theory Guide. Online document (2011)
4. Bowen, A.J., Mortensen, N.G.: Exploring the limits of WAsP. In: Proceedings of European Union Wind Energy Conference, Göteborg (1996)
5. Castro, I.P., Apsley, D.D.: Flow and dispersion over topography: a comparison between numerical and laboratory data for two-dimensional flows. In: Atmospheric Environment, vol. 31, pp. 839–850. Elsevier B.V., Amsterdam (1997)
6. Chaudhari, A.: Large-eddy simulations of wind flows over complex terrains for wind energy applications. Ph.D. thesis, Lappeenranta University of Technology (2014)
7. Chaudhari, A., Hellsten, A., Agafonova, O., Hamalainen, J.: Large eddy simulation of boundary-layer flows over two-dimensional hills. In: Fontes, M., Gunther, M., Marheineke, N. (eds.) Progress in Industrial Mathematics at ECMI 2012. Mathematics in Industry, pp. 211–218. Springer International Publishing, Berlin (2014)
8. Conan, B.: Wind resource assessment in complex terrain by wind tunnel modelling. Ph.D. thesis, Orleans University (2012)
9. Khurshudyan, L.H., Snyder, W.H., Nekrasov, L.V.: Flow and Dispersion of pollutants over two-dimensional hills. United States Environmental Protection Agency Report, EPA-600/4-8 I-067 (1981)
10. Koivuniemi, A.: Identifying and addressing sources of uncertainty in modeling wind power production. Master thesis, Lappeenranta University of Technology (2011)
11. Loureiro, J., Pinho, F., Freire, S.A.: Near wall characterization of the flow over a two-dimensional steep smooth hill. Exp. Fluids **42**(3), 441–457 (2007)
12. Wilcox, D.: Turbulence Modelling for CFD. DCW Industries Inc, La Canada (1994)